Copyright (1996) American Geophysical Union. Reproduced by permission of American Geophysical Union. Further reproduction or electronic distribution is not permitted.

GEOPHYSICAL RESEARCH LETTERS, VOL. 23, NO. 18, PAGES 2425-2428, SEPTEMBER 1, 1996

Anomalous shear strain at Parkfield during 1993-94

R.L. Gwyther, M.T. Gladwin, M. Mee and R.H.G. Hart

C.S.I.R.O. Exploration and Mining, Pinjarra Hills, QLD Australia

Abstract: Three borehole tensor strainmeters (BTSM) installed near Parkfield and separated by more than 5km have established a good baseline of data spanning the past eight years. A significant change in the accumulation rate of shear strain (0.5 and 1.0 microstrain per year at two of the sites) commencing approximately in mid-1993 and continuing to 1995 is evident in these data. Some supporting evidence for a change in the strain rate at that time is seen in dilatometer data, geodetic measurements, fault zone properties and microearthquake locations. There was also an increase in medium level seismic activity (M=4.7 on 10/20/92; M=3.9 on 10/26/92; m=3.5 on 3/13/93; M=4.4 on 4/3/93; M=4.8 on 11/14/93) in the Middle Mountain area. While a rainfall induced strain may have caused the observed strain anomaly, we propose a more likely explanation is that aseismic slip at depth on a section of the fault south of Middle Mountain produced the observed strain anomaly. This anomaly is unique in the current data set.

Introduction

The Parkfield experiment currently consists of more than 21 instrument networks including seismic networks, laser and GPS based geodetic networks, borehole strain and tilt, radon and hydrogen emissions, resistivity, magnetic field and surface creep measurements (*Roeloffs and Langbein, 1994*). Though the expected earthquake has not occurred to date, this intensive study of fault processes has shown that in spite of relatively simple fault geometry in this region, the underlying earthquake preparation process is complex and still not well understood. The initial model (*Bakun and Lindh, 1985*) of a characteristic earthquake resulting from failure of an asperity zone (*Harris and Segall, 1987*), with a periodicity of 22 years has been the subject of much debate (eg. *Ben Zion and Rice, 1993*).

Recent microearthquake and seismic velocity studies have revealed that aseismic and seismic failure processes predominate in differing regions of the fault surface (*Lees and Malin 1990, Nadeau et al., 1994*). These conclusions highlight a need for localised continuous observations of aseismic processes. Here we report on aseismic processes observed by borehole tensor strain instruments. The BTSM measures three independent horizontal strains, enabling determination of the horizontal components of the tensor strain field (ε_{yy} , ε_{yy} and ε_{xy} , in an axis system x east and y north), with a resolution of 1 nanostrain, sampling interval of 30 minutes and stability better than 100 nanostrain per year.

Three BTSM instruments were installed in the Parkfield region in late 1986, and now provide an 8 year baseline of tensor strain data. The Donalee (DLT) instrument is 3.9 km from the fault trace and at a depth of 174 m, Eades (EDT) is 0.7 km from the fault trace at a depth of 272 m, and Frolich (FLT) is situated 2.4 km from the fault at a depth of 237 m . These sites form a 6 km wide array spanning the fault trace, and are shown in Figure 1(a) together with the approximate 1966 epicentre near Middle Mountain, the town of Parkfield, and the rupture zone during the 1966 M_L 5.5 earthquake (*King et al., 1987*). Figure 1(b) is a vertical section in the fault plane, indicating the relative positions of the borehole strain and creep instruments, and the northwestern extent of the 1966 rupture surface.

Copyright 1996 by the American Geophysical Union.

Paper number 96GL02256
0094-8534/96/96GL-02256$05.00

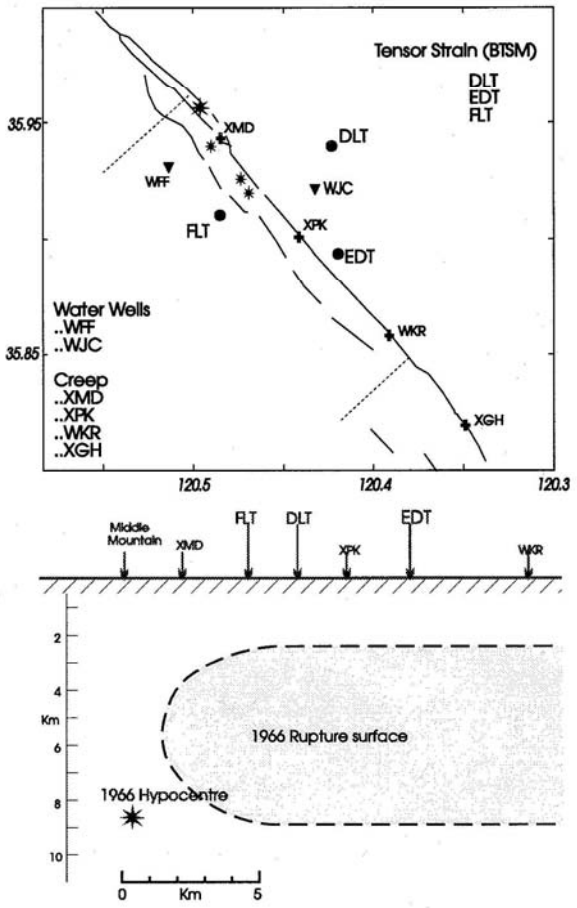

Figure 1(a). Map of the San Andreas fault trace in the region of Parkfield, showing the locations of BTSM sites (circles). Dilatometers are colocated near DLT and FLT. Surface creep sites (crosses) and water wells (triangles) are shown also. The large star shows the epicentre of the 1966 earthquake. Dotted lines show the region detailed in vertical section in Figure 1(b). Indicated are the relative positions of the borehole strain and creep instruments, and the 1966 hypocentre and rupture surface (*Harris & Segall*, 1987).

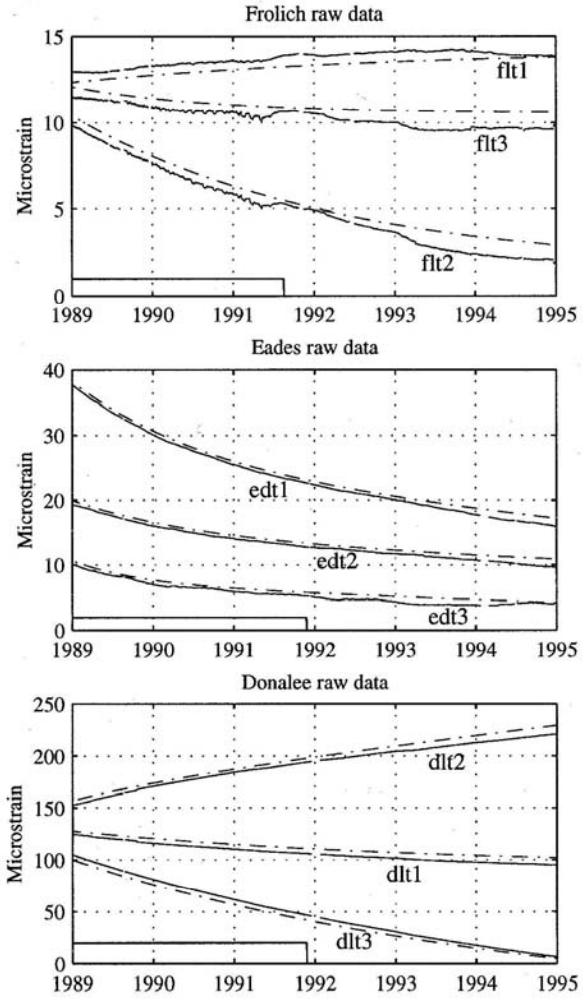

Figure 2(a), (b) &(c). Raw data from the 3 active gauges of the Frolich, Eades and Donalee tensor strain instruments, in microstrain. Decay curves fitted to each gauge dataset over the period 1988-1991 are shown dotted, slightly offset for clarity.

Raw BTSM data contain strain signals due to curing of grout as well as viscoelastic creep of the grout and rock close to the borehole. These signals can be approximated by two exponential decay functions with time constants of order 10 days, and 100 to 1000 days, respectively. Such terms are not relevant to measurement of the surrounding strain field, and are removed (see Figure 2) by non-linear least squares fitting of exponentials over the interval 1988-1991 for each strain component (*Gwyther, 1995*). The individual strain residuals are combined to determine areal strain $\varepsilon_a = \varepsilon_{xx} + \varepsilon_{yy}$ and shear strains $\gamma_1 = \varepsilon_{xx} - \varepsilon_{yy}$, and $\gamma_2 = 2\varepsilon_{xy}$, and are calibrated by estimation of borehole inclusion elastic parameters (*Gladwin and Hart, 1985*).

Tensor Strain Anomalies During 1993-1994

Residual areal strains measured by each instrument are shown in the upper part of Figure 3, and shear strains for FLT and EDT are shown in Figure 4.

In the data from the FLT instrument, an areal strain signal with a periodicity of 20 to 30 days, and an amplitude of 200 to 300 $n\varepsilon$, was present until mid 1991. After that time the character of the areal strain data altered, suggesting that the signal had been caused by local cultural activity. Excursions in the areal strain of approximately 500 $n\varepsilon$ at the end of each year correspond with increased rainfall at those times, indicating the presence of hydrologically induced areal strain in the records. FLT shear strains were relatively stable from 1989 until late 1993. A change in γ_2 shear strain rate of -500 $n\varepsilon$ per year commenced in late 1993 (with a less well defined change of +100 $n\varepsilon$ per year in γ_1 shear strain rate), and continued until October 1994. FLT shear strains during 1995 were again relatively constant

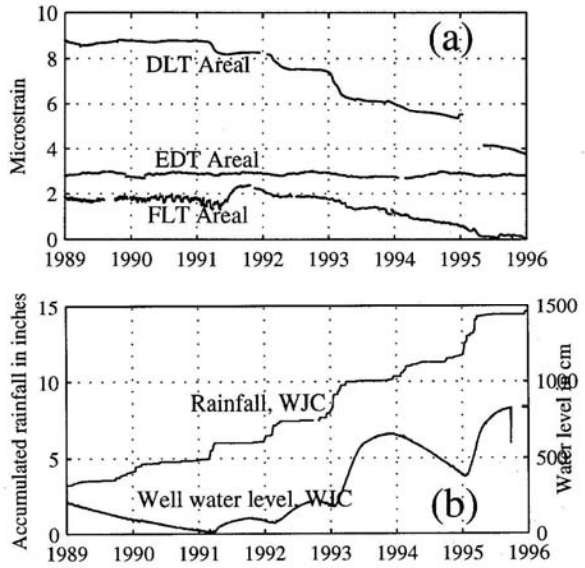

Figure 3(a). Areal strain data at each tensor strain site (compression negative). Figure 3(b) shows accumulated rainfall data measured at WJC(close to the Donalee site) from 1988 to 1994 and water level data measured at WJC.

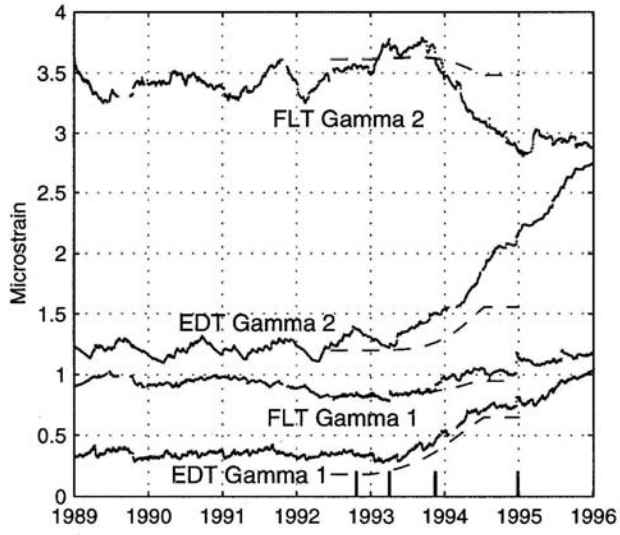

Figure 4. Observed shear strains γ_1 and γ_2 at Eades and Frolich, with modelled strains resulting from the best fit model superimposed and offset. Local earthquakes with magnitude M_L >4 occurring since 1986 are shown as heavy vertical bars in the lower part of the figure.

The Eades instrument shows shear strain data from 1989 until early 1993 having deviations of less than $\pm$ 100 $n\varepsilon$. From early 1993, a change of more than + 600 $n\varepsilon$ per year in both shear strain rates occurred. This anomaly continued until September 1994, after which the strain rates returned to the 1989-1993 rate until the December 1994 M_L4.9 earthquake. Both γ_1 and γ_2 again increased in mid 1995.

The dominant signals in the Donalee areal strain data are annual changes of order 1 to 2 microstrain in areal strain almost certainly caused by seasonal changes of pressure in a local, highly conductive and confined aquifer (*E. Roeloffs,1995, pers. comm).* Figure 3(b) shows accumulated rainfall and water level records at Joaquin Canyon (WJC) within one km of Donalee (data courtesy of *E. Roeloffs, USGS).* The correspondence of rainfall with the Donalee areal strain is clear, with a lesser degree of contamination in the Frolich areal strain data, and little influence in the Eades areal strain.

The water well data show significant changes in early 1991, 1992, 1993 and 1995, with recharge of the aquifer during 1994 after the long period of effective drought from 1986 until 1994. Water level changes are caused by both dilatational strain as well as changes in aquifer pressure initiated by rainfall (*Roeloffs*, 1988), and it is difficult to separate out these two influences. The strains associated with these hydrological influences are not limited to areal strain, and shear strains are also contaminated in the Donalee data at a level of a few hundred nanostrain. Consequently the Donalee strain data and areal strains from Eades and Frolich were not used as constraints in the modelling. The shear strain data at the latter two sites show no influence of hydrological effects at a level greater than $\pm$ 100 $n\varepsilon$ (see Figure 4). Our examination of the two data sets indicates that the shear strain data at EDT and FLT do not show a linear admittance to the full 7 year record of either accumulated rainfall, water well WJC level, or the first derivative of this level. In view of this, and since the significant difference in time signatures of strain at EDT and FLT over 1994/95 suggests a cause other than rainfall induced strain, we suggest that it is unlikely that the anomaly is totally caused by rainfall-induced aquifer pressure changes or associated thermoelastic effects. Consequently we investigated possible fault slip models.

Model Of Propagating Aseismic Slip

The anomaly in the shear strains at Eades and Frolich shown in Figure 4 is consistent with a source propagating from the southeast along the fault towards the northwest. The Eades anomaly commenced in early 1993, while the Frolich anomaly commenced approximately six to nine months later. The propagation time suggests aseismic slip at depth occurring progressively along the fault.

Propagating sources were modelled as a uniformly timed series of simple rectangular dislocation surfaces with appropriate dimensions, amount of slip, and relative position (*Okada, 1985).* The strains at the instrument sites due to slip on each surface were summed to derive a time history. The slip surfaces were constrained to the fault plane with a uniform progression rate of 3 km per year. A range of propagating directions of aseismic slip were considered, including vertical and along-strike propagation of slip patches, and an expanding slip surface initiating at depth and growing to the northwest. For the geometry of each case considered, a slip history on each surface was input as a further variable. An a priori slip rate history was chosen to increase from zero to a maximum and back to zero over the course of the propagation sequence.

The best model derived from the above analysis is aseismic slip initiating in a rectangular region at a depth of 4 km, with a length of 4 km and width 1 km, centred below the projection of Eades on the fault trace. Medium term noise in the data (± 100 nanostrain) precludes specification of these parameters at better than ± 0.5 km. Slip then propagated both towards the surface and northwest along the fault, with a final upper limit at depth 1 km below the Frolich site. The slip experienced by any section of the fault surface during this process was equivalent to 20 mm per year, extending over a period of 5 months. A diagram of this modelled fault behaviour is illustrated in Figure 5, with the projections of stations shown at the top. Modelled shear strain data is shown as dotted curves in Figure 4. Modelled areal strains are not directly comparable with observed areal strains because of the greater influence of hydrological factors.

Discussion

Seismic activity in the region increased during 1993 and 1994, with the only four M_L>4 events since 1986 occurring between October 1992 and December 1994 (*U.S.G.S. CALNET catalog*). The locations of these four events are shown as stars in Figure 1(a), and as vertical bars on the plot of BTSM shear strain anomalies in Figure 4. The coincidence of this medium level seismicity with the 1993-1994 anomaly can be seen clearly. Other instrument data measured at Parkfield also indicate anomalous signals in 1993-94, in particular borehole dilatometer observations (*USGS dataset, per fav. M.J.S. Johnston*), geodetic measurements (*Langbein, 1995*), low frequency electromagnetic field measurements (*Teague et al., 1994),* fault zone elastic properties (*Karageorgi, 1994*) and microearthquake locations (*Malin, 1996, ms. in review*). None of these data sets has been used to constrain of the models described above, and a joint investigation of all relevant datasets is a high priority.

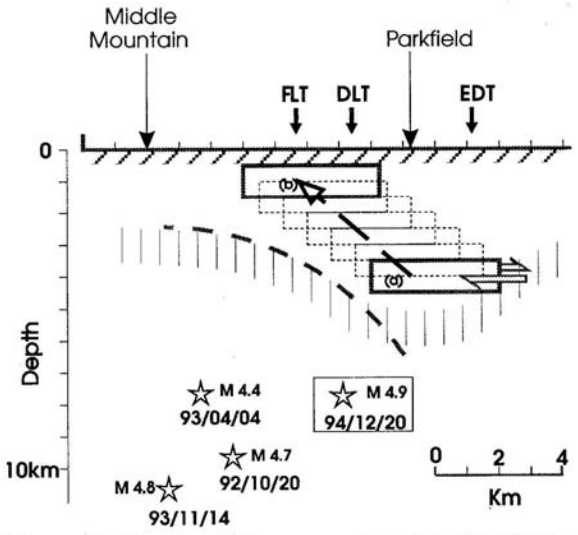

Figure 5. Diagram of the proposed model of aseismic slip propagation, shown in fault cross section. Hypocentres of the three earthquakes larger than M_L 4 to occur since 1986 are shown. Dotted circular line indicates a suggested region of stress relaxation. Measured microearthquake activity (*Malin and Alverez, 1992*) occurred mainly below the vertically shaded region shown.

The proposed aseismic slip model is consistent with results of two recent studies of microearthquake activity observed with a 10 station, high resolution, downhole seismic network installed around the Parkfield region. *Nadeau et al.* (*1994*) reported clustering of microearthquakes at predominantly shallow depths, and propagation between clusters. *Malin and Alvarez* (1992) identified a zone in the upper 5km to the southeast of Middle Mountain which has little seismic activity. The correspondence of this zone of low microseismic activity with the modelled aseismic slip patch is striking. It is possible that the microearthquake propagation and tensor strain anomalies are actually observations of different but complementary processes: the **microearthquake activity** propagating northwest from Frolich, at depths 3 - 10 km (*Malin, 1996, ms. in review*), and concurrent **aseismic slip** with very little brittle microearthquake activity occurring in the modelled zone and propagating from Eades towards Frolich.

A possible mechanism for the process leading to the modelled aseismic slip shown diagramatically in Figure 5 can be described: Stress release during the three M_L ~ 4 earthquakes in 1992-93 led to release of strain in a region shown by the circular dotted line in Figure 5, causing increased stresses on the boundary of that region. This increased stress triggered aseismic failure in the modelled patches, and is consistent with the microearthquake activity, which documents the readjustment of stress in the brittle zone surrounding the earthquake sources.

A M_L 4.9 earthquake occurred southeast of Middle Mountain on 20 December 1994, and the projection of its hypocentre onto the fault plane is shown in Figure 5. This was the largest earthquake to occur in more than 10 years along this section of the fault. Its epicentre was well to the southeast of the preparation zone of the 1934 and 1966 Parkfield earthquakes, which is close to Middle Mountain. The uniqueness of this earthquake leads to the question of whether the anomalies observed in 1993 - 94 were precursors to the event. The processes of stress readjustment to the northwest (by microearthquake activity) and directly above (by aseismic slip) are at least consistent with an increased stress leading to failure on a surface centred at this location. Furthermore the hypocentre is situated in the region of low microearthquake activity identified and suggested as a possible future site for moderate earthquakes (see Figure 1 of *Malin and Alvarez* ,1992). Further observations of detailed fault properties from downhole seismic investigations of vibroseis data are necessary before more refined models can be made.

In conclusion, clear anomalies in shear strain accumulation rates at Eades and Frolich during 1993 - 1994 are supported by anomalous data observed on a range of other instrument types. The data suggest a wide scale regional anomaly during this period. A model of aseismic slip propagating simultaneously towards the surface and towards the northwest from Eades to Frolich has been derived from the BTSM data alone. This aseismic slip zone forms a complementary geometry with the zone in which microearthquake activity propagated during the same time interval. We propose that brittle failure by microearthquakes and slow aseismic slip are complementary mechanisms for accomodating stress in the transitional zone of the San Andreas fault from Parkfield to Middle Mountain

Acknowledgements. This work was performed with support from the U. S. Geological Survey, Department of the Interior under the National Earthquake Hazards Reduction Program. Contents do not represent policy of that agency,and no endorsement of the agency is to be assumed. The borehole tensor strain instrument was previously developed under awards of the Australian Research Grants Scheme, and fabricated by R. Willoby and staff in house. We thank R. Liechti for maintenance support, Kate Breckenridge for data support, and A. Linde and M. Johnston for support in the program.

References

Bakun W.H. and Lindh A.G., The Parkfield California Earthquake Prediction Experiment, *Science*, 229, 619-623, 1985.

Ben Zion Y. and J.R. Rice, Earthquake Failure Sequences along a Cellular Fault Zone in a Three-Dimensional Elastic Solid Containing Asperity and Nonasperity Regions, *J. Geophys. Res. 98(B8),* 14109-14131, 1993.

Gladwin, M. T., High Precision multi component borehole deformation monitoring. *Rev.Sci.Instrum.*, 55, 2011-2016, 1984.

Gladwin M.T. and R. Hart, Design Parameters for Borehole Strain Instrumentation, *PAGEOPH, 123*, 59-80, 1985.

Gwyther R.L., M.T. Gladwin and M.M.Mee A Continuing Regional Strain Anomaly Observed on Parkfield Borehole Tensor Strain Array *EOS Trans. A.G.U.* 75(44), 438, 1994

Gwyther R.L. An Investigation of Aseismic Fault Processes in California with Borehole Strain Measurements. *PhD Thesis*, Brisbane, Australia.

Harris R.A. and P. Segall Detection of a Locked Zone at Depth on the Parkfield, California, Segment of the San Andreas Fault *J. Geophys. Res.* 92(B8), 7945-7962, 1987

Karageorgi E.D., T.V. McEvilly and R.W. Clymer Parkfield Prediction Experiment:Update on Monitoring with Repeated Vibroseis Sources *EOS Trans. A.G.U.* 75(44), 471, 1994

King N.E., P. Segall and W. Prescott Geodetic Measurements near Parkfield, California, 1959-1984 *J. Geophys. Res., 92(B3),* 2533-2552, 1987

Langbein, J.O. Geodetic Strain Monitoring *U.S.G.S. Summ. Tech. Rep. XXXVI*, O.F.R.95-210, 514, 1995

Lees J.M. and P.E. Malin Tomographic Images of P Wave Velocity Variation at Parkfield, California *J. Geophys. Res.*, 95(B13)\, 21793-21804, 1990

Malin P.E., S.N. Blakeslee, M.G. Alvarez and A.J. Martin Microearthquake Imaging of the Parkfield Asperity *Science* 244, 557-559, 1989

Malin P.E. and M.G. Alvarez Stress Diffusion Along the San Andreas Fault, Parkfield, California *Science* 256, 1005-1007, 1992

Nadeau R., M. Antolik, P.A. Johnson, W. Foxall and T.V. McEvilly Seismological Studies at Parkfield. III. Microearthquake Clusters in the Study of Fault Zone Dynamics *Bull. Seis. Soc. Am.* 84(2), 247-263, 1994

Okada, Y., Surface Deformation due to Shear and Tensile Faults in a Half-Space. *Bull. Seis. Soc. Am.* 75 (4) 1435-1454, 1985.

Roeloffs E.A. Hydrologic Precursors to Earthquakes: A Review *PAGEOPH*, 126(2-4), 177-209, 1988

Roeloffs E. and J. Langbein The Earthquake Prediction Experiment, Parkfield, California. *Rev. Geophys* 32(3), 315-336, 1994

Teague C., M. Johnston, A. Fraser-Smith, P. McGill, R. Mueller and W. Wiegand Anomalous ULF Signals at Parkfield During the Period December 1993 to May 1994 *EOS Trans. A.G.U.* 75(44), 470, 1994

R.Gwyther, C.S.I.R.O., 2643 Moggill Rd., Pinjarra Hills, QLD 4069 Australia (email: r.gwyther@dem.csiro.au)

M.T. Gladwin, C.S.I.R.O., 2643 Moggill Rd., Pinjarra Hills, QLD 4069 Australia (email: m.gladwin@dem.csiro.au)

R. Hart, C.S.I.R.O., 2643 Moggill Rd., Pinjarra Hills, QLD 4069 Australia (email: r.hart@dem.csiro.au)

M. Mee, C.S.I.R.O., 2643 Moggill Rd., Pinjarra Hills, QLD 4069 Australia (email: m.mee@dem.csiro.au)

(Received December 6, 1996; revised March 14, 1996; accepted July 10, 1996)